

Kinetics and mechanism of formation of monocalcium aluminate, CaAl_2O_4

Beshir M. Mohamed and John H. Sharp

Department of Engineering Materials, University of Sheffield, Mappin Street, Sheffield, UK S1 3JD

The kinetics of the reaction for the formation of monocalcium aluminate (CaAl_2O_4) using 1 : 1 molar mixtures of A.R. grade calcium carbonate and A.R. $\alpha\text{-Al}_2\text{O}_3$ or gibbsite have been investigated in the range 1150–1400 °C using quantitative X-ray diffraction analysis. The phases $\text{Ca}_3\text{Al}_2\text{O}_6$ and $\text{Ca}_{12}\text{Al}_{14}\text{O}_{33}$ were found to be intermediates in the formation of CaAl_2O_4 , whereas CaAl_4O_7 was formed *via* an initial side reaction. The formation of CaAl_2O_4 from the oxides was found to fit well with the diffusion controlled model of Ginstling and Brounshtein. The activation energy for the formation of CaAl_2O_4 from the amount of CaAl_2O_4 formed from the reaction of calcite with $\alpha\text{-Al}_2\text{O}_3$ was determined to be $205 \pm 10 \text{ kJ mol}^{-1}$.

Monocalcium aluminate, CaAl_2O_4 (or CA), is the main constituent found in calcium aluminate cements used in a wide range of applications in the construction and mining industries and especially in refractory castables for the steel industry.¹ Recently calcium aluminates have also been used in applications in optical and structural ceramics. Goktas and Weinberg² and Wallenberger *et al.*³ indicated that some amorphous calcium aluminate compositions are photosensitive, and therefore potential candidates for optical information storage devices. They also have very desirable IR transmission properties for optical fibre applications. Crystalline calcium aluminates are also used in high-strength and high-toughness polymer-modified cement-based materials.⁴

The use of calcium aluminate cements in refractory applications still dominates their other uses. Control of the method of production is of importance to improve the service properties of refractory concretes based on these cements. Commercial production of the most refractory calcium aluminate cements with 70–80% Al_2O_3 contents takes place in a kiln by a solid-state sintering process. Inevitably equilibrium is not reached and a heterogeneous reaction product is formed containing CA and CA_2 ($\text{C}=\text{CaO}$, $\text{A}=\text{Al}_2\text{O}_3$) as major phases, with C_{12}A_7 and unreacted $\alpha\text{-Al}_2\text{O}_3$ as minor phases. It is important to know about the kinetics of formation of these phases and their sequence of formation to understand better the reactions that take place in the kiln. The synthesis of monocalcium aluminate, which is the principal phase in all the calcium aluminate cements, is the subject of this paper.

There is confusion in the literature in that the intermediates reported by different workers in the process of formation of monocalcium aluminate were often different and the activation energies reported varied considerably. Williamson and Glasser⁵ reported that $\text{Ca}_3\text{Al}_2\text{O}_6$ (C_3A) and $\text{Ca}_{12}\text{Al}_{14}\text{O}_{33}$ (C_{12}A_7) are intermediates in the formation of CaAl_2O_4 , but later workers disagreed with them. For example, Scian *et al.*⁶ included CaAl_4O_7 (CA_2) as another intermediate phase, while Singh *et al.*⁷ reported that $\text{Ca}_3\text{Al}_2\text{O}_6$, $\text{Ca}_{12}\text{Al}_{14}\text{O}_{33}$, CaAl_4O_7 and $\text{CaAl}_{12}\text{O}_{19}$ (CA_6) could all be formed as intermediate phases.

Similar confusion relates to the magnitude of the activation energy for the formation of CaAl_2O_4 with values reported of $151.5 \text{ kJ mol}^{-1}$ (Repenko⁸), 303 kJ mol^{-1} (Scian *et al.*⁶) and 376 kJ mol^{-1} (Chou and Burnet⁹). It is, therefore, timely to reinvestigate the kinetics and mechanism of formation of monocalcium aluminate.

Experimental

The required amounts for the 1 : 1 molar proportions of A. R. calcite and A. R. $\alpha\text{-alumina}$ or gibbsite, $\text{Al}(\text{OH})_3$, were accu-

rately weighed out to four decimal places and intimately mixed using boiled distilled water. The slurry was filtered using a vacuum pump and dried in an oven at 110 °C. Pellets (1 g each), with a diameter of about 12.5 mm, were made from each mixture by single-ended pressing using a steel die. Press loading of 326 MPa was used throughout the experiments.

The pellets of the sample were fired in a sintered alumina boat. They were normally heated to about 900 °C for 1 h to allow for evolution of CO_2 without the formation of any calcium aluminate phase and then pushed into the hot firing zone. The reactions between calcium oxide and $\alpha\text{-Al}_2\text{O}_3$ or $\text{Al}(\text{OH})_3$ were studied at 1150, 1200, 1250, 1300, 1350 and 1400 °C for 0.5–24 h. After each run the alumina boat containing the pellets was removed quickly from the furnace, a sample taken and the boat pushed back into the hot zone. The fired samples were quenched in air, stored in plastic bags and kept in a desiccator to be analysed by the X-ray diffraction technique.

To determine the calcium aluminate phases present quantitatively in each reaction mixture after firing, the X-ray diffraction method was used. To do this, the quenched fired samples were ground using a mechanically driven agate mortar to pass a 38 μm sieve before the analysis. To eliminate the preferred orientation problem which may affect the analysis, randomly orientated samples were prepared by the back loading technique.¹⁰ The fractions of all the reaction products formed during the reactions were quantitatively determined by XRD using the internal standard method. Rutile (TiO_2) was chosen as the internal standard. The peaks used for the QXRD analysis are shown in Table 1. A calibration curve was determined from pure, laboratory synthesised monocalcium aluminate, made from calcite and $\alpha\text{-Al}_2\text{O}_3$ at 1450 °C, fired three times with intermediate grinding.

Table 1 Reference peaks used for quantitative determination of the calcium aluminate phases

phase	Miller index, hkl	$d/\text{\AA}$	2θ	relative intensity	disturbing phase
$\alpha\text{-Al}_2\text{O}_3$	113	2.085	43.36	100	—
	024	1.740	52.55	45	—
rutile	110	3.247	27.44	100	—
C_3A	440	2.699	33.16	100	C_{12}A_7
C_3A	800	1.909	47.6	45	—
C_{12}A_7	211	4.89	18.13	95	—
CA	220	2.966	30.10	100	C_{12}A_7
CA	112	4.67	19.00	25	—
CA_2	020	4.44	19.98	55	—
CA_6	0110	2.007	45.14	60	—
CA_6	1112	1.533	60.32	65	—

Results and Discussion

Intermediate phases formed in the reaction between calcite and α - Al_2O_3

The amount of CaAl_2O_4 formed over times in the range 0.5–24 h was dependent on the firing temperature, as shown in Fig. 1, which demonstrates that this amount always increased with increase in temperature. At 1150 °C, the time taken to reach half reaction was about 24 h, whereas at 1400 °C it was only about 30 min.

Monocalcium aluminate was not, however, the only phase formed at the temperatures of investigation. Three other calcium aluminate phases were also observed, as shown in Fig. 2.

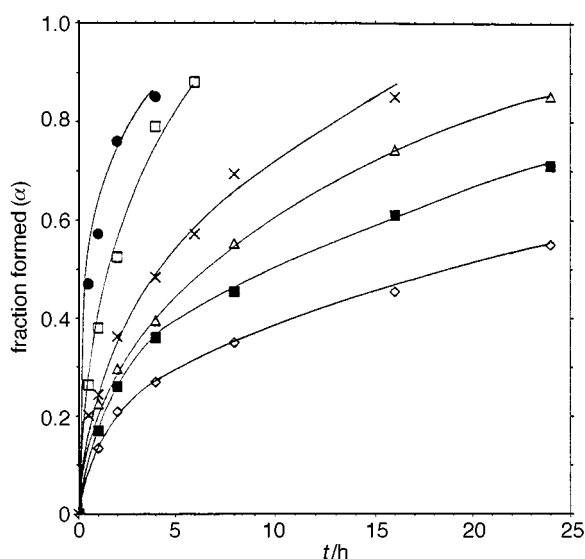


Fig. 1 Plots of fraction of CA formed vs. time at $T=1150$ (\diamond), 1200 (\blacksquare), 1250 (\triangle), 1300 (\times), 1350 (\square), 1400 °C (\bullet)

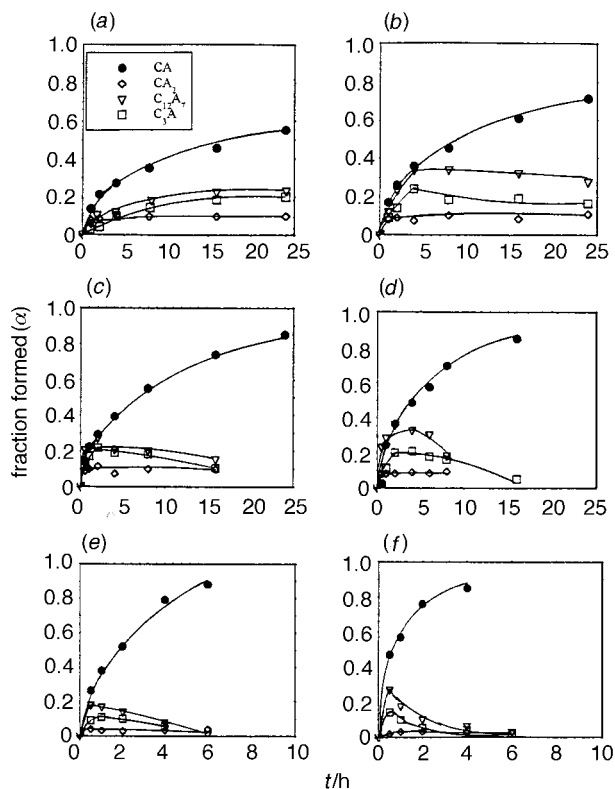


Fig. 2 Formation of the various calcium aluminate phases (\bullet , CA; \diamond , CA_2 ; ∇ , C_{12}A_7 ; \square , C_3A) during the synthesis of CA at (a) 1150, (b) 1200, (c) 1250, (d) 1300, (e) 1350, (f) 1400 °C

It can be seen from the data shown in Fig. 2(a) that at 1150 °C, the amount of $\text{Ca}_3\text{Al}_2\text{O}_6$ formed increased with increasing time for 8 h and then remained almost constant up to 24 h. A similar trend of behaviour applied to the formation of the $\text{Ca}_{12}\text{Al}_{14}\text{O}_{33}$ and CaAl_4O_7 phases. Unreacted CaO was also present.

At higher temperatures, 1200, 1250, 1300, 1350 and 1400 °C as shown in Fig. 2(b)–(f), the amount of CaAl_2O_4 always increased with increasing time, whereas the amounts of $\text{Ca}_3\text{Al}_2\text{O}_6$ and $\text{Ca}_{12}\text{Al}_{14}\text{O}_{33}$ initially increased with time, but after reaching a maximum value the amounts of these phases subsequently decreased with increasing time. The higher the temperature, the shorter the time to reach the maximum before the amounts of $\text{Ca}_{12}\text{Al}_{14}\text{O}_{33}$ and $\text{Ca}_3\text{Al}_2\text{O}_6$ present started to decrease. The behaviour of CaAl_4O_7 was, however, different. It was observed at all temperatures investigated, but only in relatively small amounts, which remained approximately constant with increasing time after its initial formation.

It can be seen that all the compounds in the system $\text{CaO}-\text{Al}_2\text{O}_3$ were formed except for $\text{CaAl}_{12}\text{O}_{19}$, which was not detected even at the highest temperature (1400 °C) of firing in this study. It can be seen from Fig. 2(a) that the $\text{Ca}_3\text{Al}_2\text{O}_6$ and the $\text{Ca}_{12}\text{Al}_{14}\text{O}_{33}$ phases were still present at 1150 °C even after 24 h, because of the continued presence of CaO in the system. At 1400 °C, these phases had almost disappeared after 6 h.

Even when most of the α - Al_2O_3 had reacted at 1150 °C, the formation of CaAl_2O_4 was very sluggish, in part because the intermediates formed from the starting materials at the expense of CaAl_2O_4 , and in part because of the slow conversion of these phases to form CaAl_2O_4 at such a low temperature.

The XRD analysis of the fired samples at 1200 °C indicated that CaO was present for the first 16 h, whereas at 1250 and 1300 °C it was observed for only about 1 h. At higher temperatures there was no indication of the presence of CaO in any of the reaction products.

At 1400 °C there was no sign of any unreacted alumina either. $\text{Ca}_3\text{Al}_2\text{O}_6$ and $\text{Ca}_{12}\text{Al}_{14}\text{O}_{33}$ were formed in small amounts and reacted after a short time, which confirmed that these phases were intermediates in the formation of CaAl_2O_4 . CaAl_4O_7 was initially formed in small amounts and remained approximately constant with increasing time at all temperatures investigated.

It is expected from the binary phase diagram for the $\text{CaO}-\text{Al}_2\text{O}_3$ system that liquid will be formed at 1400 °C and this was confirmed by microstructural observation. Hence the amount of CaAl_2O_4 formed initially was very high (about 50% in 30 min). The composition of the liquid phase changes as the $\text{Ca}_{12}\text{Al}_{14}\text{O}_{33}$ reaction intermediate is consumed.

The general behaviour of $\text{Ca}_3\text{Al}_2\text{O}_6$ at all the temperatures investigated was that it was formed as an intermediate as indicated by its decrease with increasing time. $\text{Ca}_{12}\text{Al}_{14}\text{O}_{33}$ showed an increase limited by the time and temperature of reaction, reaching a maximum value, followed by a decrease, confirming that it was also formed as an intermediate phase. On the other hand, the almost constant amount of CaAl_4O_7 formed with increasing time at all temperatures investigated suggests that it was formed by a side-reaction and was not a reaction intermediate.

Kinetics of the reaction between calcite and α - Al_2O_3

The kinetic mechanism for the reaction of 1:1 C:A to form CaAl_2O_4 was analysed from the amount of CaAl_2O_4 formed, using the master curve¹¹ of fraction reacted α against reduced time. Although $t/t_{0.5}$ has been frequently used in the literature, $t/t_{0.3}$ has been used in Fig. 3 to test for the reaction mechanism involved, since it discriminates more at high values of α when the experimental data are sufficiently reliable. The time to achieve 30% conversion was determined from the plots of α vs. t shown in Fig. 1 at the reaction temperatures investigated.

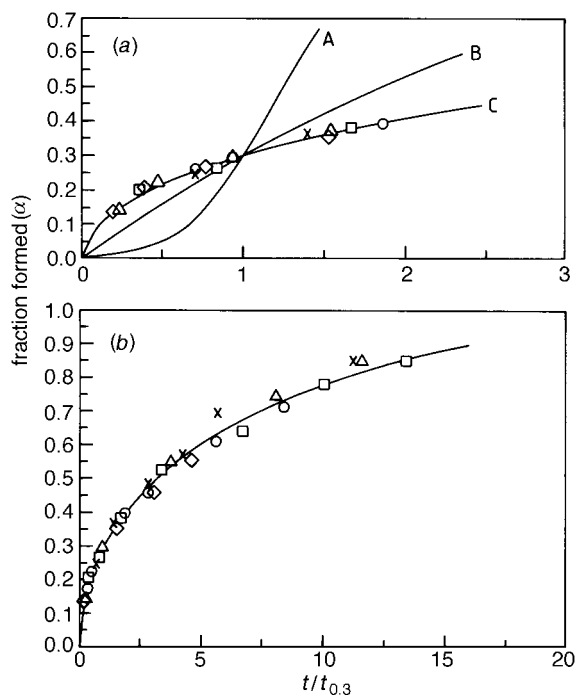


Fig. 3 Reduced time plots of the formation of CA vs. $t/t_{0.3}$ (\diamond , 1150; \circ , 1200; \triangle , 1250; \times , 1300; \square , 1350 °C). Calculated curves drawn for (A) $A_3(\alpha)$, (B) $R_3(\alpha)$, (C) $D_4(\alpha)$, see text.

From Fig. 3(a) it can be seen that: (1) all experimental data are isokinetic, *i.e.* they follow the same curve and (2) the experimental data follow curve C rather than curves A or B.

The data shown in Fig. 3(b) show that this relationship is followed up to very high values of α . The three curves, A, B and C, are calculated from different kinetic models. In each case it is assumed that the reaction is taking place in three dimensions. The first model is based on the Avrami-Erofe'ev equation^{12,13} for nucleation and growth:

$$A_3(\alpha) = [-\ln(1-\alpha)]^{1/3} = kt$$

The second model is based on the movement of a reaction interface into a spherical particle:¹¹

$$R_3(\alpha) = 1 - (1-\alpha)^{1/3} = kt$$

The third model is that developed for a three-dimensional diffusion controlled reaction by Ginstling and Brounshtein:¹⁴

$$D_4(\alpha) = 1 - 2\alpha/3 - (1-\alpha)^{2/3} = kt$$

The data clearly fit very well with the calculated data based on Ginstling and Brounshtein's¹⁴ equation. The curve shown in Fig. 3 is not that through the experimental data, but that calculated for ideal data following the mechanism of Ginstling and Brounshtein. The agreement between the experimental and calculated data is good and continues to a fraction reacted of at least 0.85 at the highest temperatures studied.

The method of Hancock and Sharp¹⁵ was also used to determine the kinetic mechanism from the fraction CaAl_2O_4 formed from the 1:1 C:A reaction. The $\ln\{-\ln(1-\alpha)\}$ vs. $\ln t$ plots shown in Fig. 4 give a set of good straight lines in the range of α from 0.15 to 0.57, which is that recommended for use.¹⁵ The lines drawn all have a slope of 0.57, which corresponds with that calculated from the Ginstling and Brounshtein equation, $D_4(\alpha)$. They are not an attempt to draw the best fit lines, but they do indicate an excellent fit with this mechanism. From these plots the reactions in the temperature range from 1150 to 1300 °C are shown to be isokinetic. Both the reduced time method and the \ln - \ln method confirm that the reaction of 1:1 C:A to form CaAl_2O_4 fits well with the diffusion

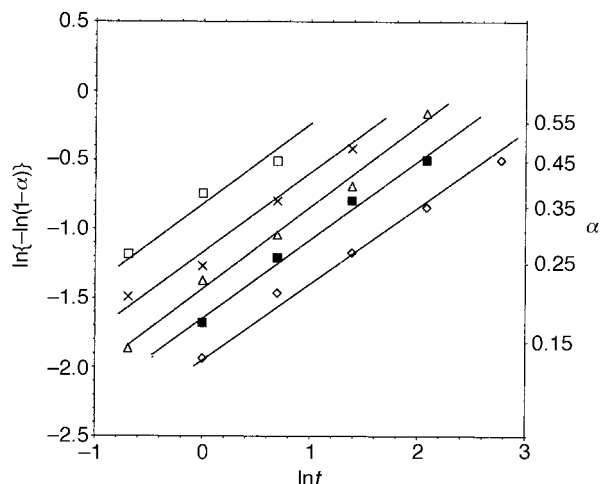


Fig. 4 \ln - \ln plots¹⁵ for the formation of CA (\diamond , 1150; \blacksquare , 1200; \triangle , 1250; \times , 1300; \square , 1350 °C)

controlled model of Ginstling and Brounshtein:

$$D_4(\alpha) = 1 - 2/3\alpha - (1-\alpha)^{2/3} = kt$$

Plots of the Ginstling and Brounshtein function, $D_4(\alpha)$, vs. time at various temperatures are shown in Fig. 5. The linearity of these plots was taken as a measure of the best fit. These lines were drawn from the data at 1150–1350 °C, but not at 1400 °C due to the liquid formation and hence data obtained at this temperature were not used in the Arrhenius plot. From the slopes of these lines, rate constants were determined at each temperature. These were then used to construct the Arrhenius plot of $\ln k$ vs. $1/T$ which is shown in Fig. 6. From the slope of this line the activation energy for the formation of CaAl_2O_4 from the amount of CaAl_2O_4 formed was determined to be $205 \pm 10 \text{ kJ mol}^{-1}$ and the pre-exponential factor, determined from the intercept, was $5.9 \times 10^8 \text{ s}^{-1}$.

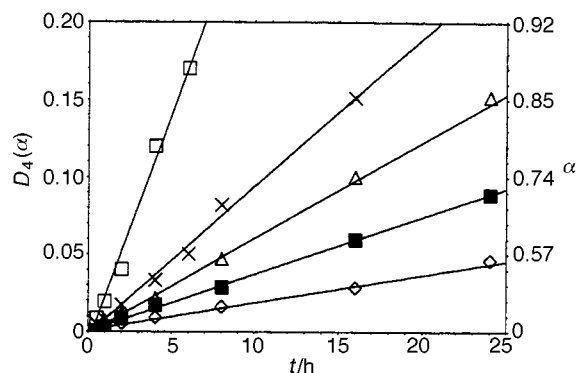


Fig. 5 Plots of $D_4(\alpha)$ vs. time for the formation of CA (\diamond , 1150; \blacksquare , 1200; \triangle , 1250; \times , 1300; \square , 1350 °C)

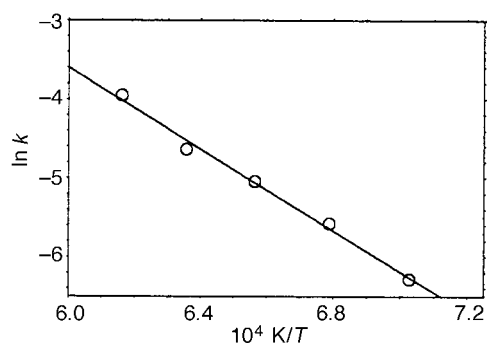


Fig. 6 Arrhenius plot for the synthesis of CA from its constituent oxides

Kinetics of the reaction between calcite and gibbsite

The sequence of formation of the calcium aluminates phases formed, *viz.* $\text{Ca}_3\text{Al}_2\text{O}_6$, $\text{Ca}_{12}\text{Al}_{14}\text{O}_{33}$ and CaAl_4O_7 , during the reaction of calcite and gibbsite to form CaAl_2O_4 was similar to that observed in the reaction between calcite and $\alpha\text{-Al}_2\text{O}_3$. $\text{Ca}_3\text{Al}_2\text{O}_6$ and $\text{Ca}_{12}\text{Al}_{14}\text{O}_{33}$ were observed at all the temperatures investigated. It is concluded that they were present as intermediate phases as indicated by their decrease with increasing time. The almost constant amount of CaAl_4O_7 formed, on the other hand, suggests that it was formed by an initial side-reaction.

A plot of fraction reacted for the synthesis of CA *vs.* time is shown in Fig. 7. The reaction was followed at six temperatures in the range from 1150 to 1400 °C. The reduced time master curve of fraction of CaAl_2O_4 formed (α) against $t/t_{0.5}$ is shown in Fig. 8 and was first used to test for the reaction mechanism involved. It can be seen that the distribution of the data at each temperature seems to fit well when compared to the master curve of α against $t/t_{0.5}$ for Ginstling and Brounshtein's diffusion model at α up to 0.5, but at higher values of α there was more scatter than when α -alumina was used. This scatter was even more evident when α was plotted against $t/t_{0.3}$.

The method of Hancock and Sharp¹⁵ was also used to determine the kinetic mechanism from the fraction of CaAl_2O_4

formed from the 1:1 C:A reaction. The $\ln\{-\ln(1-\alpha)\}$ *vs.* $\ln t$ plots shown in Fig. 9 give a set of straight lines that all have an average slope of 0.50, which corresponds reasonably well with the calculated value of 0.57 for the Ginstling and Brounshtein equation, $D_4(\alpha)$. The scatter of data points indicates less satisfactory agreement with the kinetic model than when $\alpha\text{-Al}_2\text{O}_3$ was used as the reactant.

The plots of Ginstling and Brounshtein's function, $D_4(\alpha)$, *vs.* time are shown in Fig. 10. From the slopes of these lines, rate constants were determined at each temperature, except 1400 °C. These were used to construct an Arrhenius plot of $\ln k$ *vs.* $1/T$ which is shown in Fig. 11. From the slope of this line the

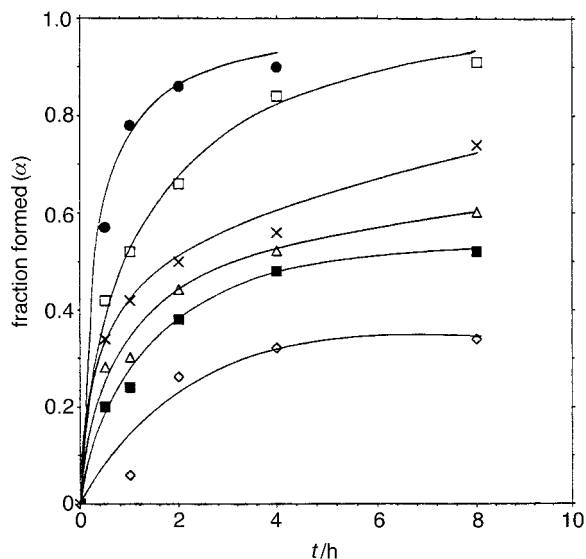


Fig. 7 Plots of fraction of CA formed from calcite and gibbsite *vs.* time at $T=1150$ (\diamond), 1200 (\blacksquare), 1250 (\triangle), 1300 (\times), 1350 (\square), 1400 °C (\bullet)

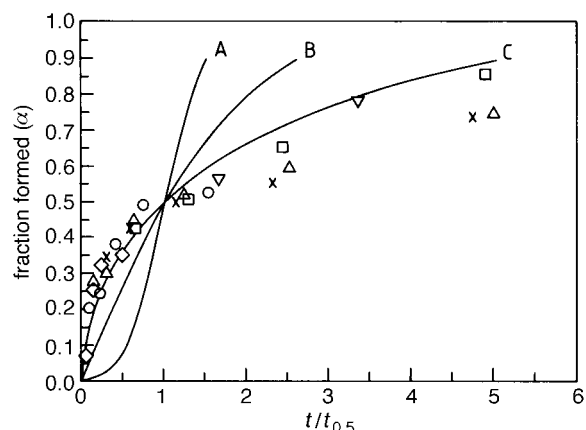


Fig. 8 Reduced time plots of the formation of CA from calcite and gibbsite *vs.* $t/t_{0.5}$ (\diamond , 1150; \circ , 1200; \triangle , 1250; \times , 1300; \square , 1350; ∇ , 1400 °C). Calculated curves drawn for (A) $A_3(\alpha)$, (B) $R_3(\alpha)$, (C) $D_4(\alpha)$.

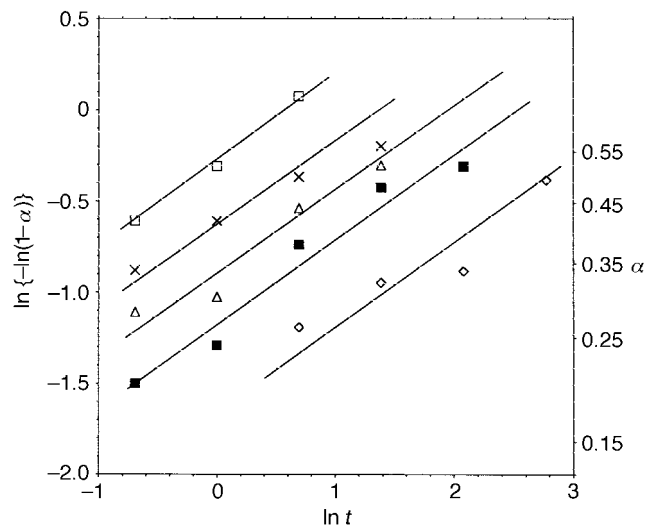


Fig. 9 $\ln\text{-}\ln$ plots¹⁵ for the formation of CA from calcite and gibbsite (\diamond , 1150; \blacksquare , 1200; \triangle , 1250; \times , 1300; \square , 1350 °C)

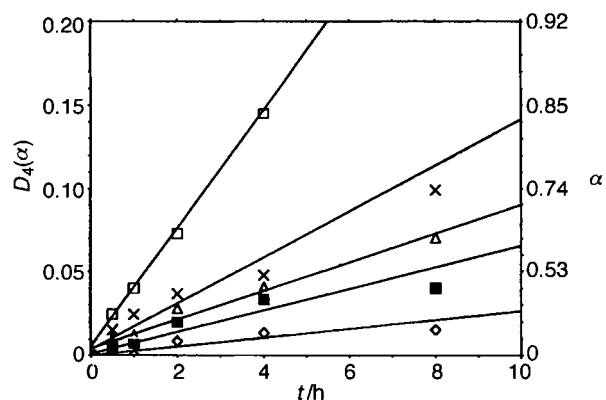


Fig. 10 Plots of $D_4(\alpha)$ *vs.* time for the formation of CA from calcite and gibbsite (\diamond , 1150; \blacksquare , 1200; \triangle , 1250; \times , 1300; \square , 1350 °C)

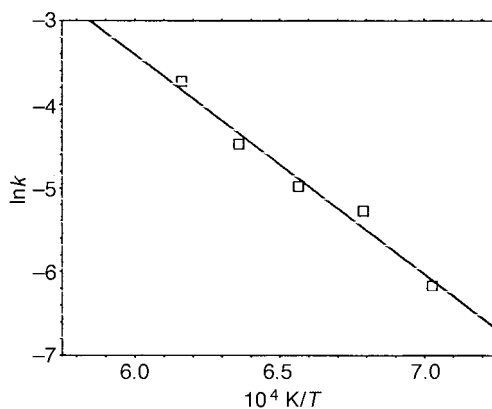


Fig. 11 Arrhenius plot for the synthesis of CA from calcite and gibbsite

activation energy for the formation of CaAl_2O_4 was determined to be 215 ± 15 kJ mol⁻¹, in close agreement with the value of 205 kJ mol⁻¹ obtained from the reaction between calcite and $\alpha\text{-Al}_2\text{O}_3$. The pre-exponential constant was determined to be 1.3×10^9 s⁻¹. Because of the less scattered kinetic data obtained when $\alpha\text{-Al}_2\text{O}_3$ was used, the value of 205 kJ mol⁻¹ is considered to be the better estimate of the activation energy for the formation of monocalcium aluminate.

Final discussion and conclusions

(1) The phases $\text{Ca}_3\text{Al}_2\text{O}_6$ and $\text{Ca}_{12}\text{Al}_{14}\text{O}_{33}$ are observed as reaction intermediates in the synthesis of CaAl_2O_4 as their amounts decrease with increasing time at constant temperature.

(2) CaAl_4O_7 is not an intermediate, but is formed through an initial side reaction.

(3) Conclusions (1) and (2) are in close agreement with the observations made by Williamson and Glasser⁵ more than 30 years ago. Later studies on the formation of intermediates are in our opinion less reliable.

(4) The kinetics of formation of CaAl_2O_4 from the oxides fit well with the diffusion controlled model of Ginstling and Brounshtein.

(5) The value of the activation energy obtained for the formation of CaAl_2O_4 from $\alpha\text{-Al}_2\text{O}_3$ and calcite (205 ± 10 kJ mol⁻¹) or gibbsite and calcite (215 ± 15 kJ mol⁻¹) are in good agreement with each other.

(6) The value of the activation energy for formation of CaAl_2O_4 (205 kJ mol⁻¹) is in the same range as that for the self diffusion of Ca^{2+} into CaO^{16} (146–268 kJ mol⁻¹), hence the rate of formation of CaAl_2O_4 is probably controlled by the rate of diffusion of Ca^{2+} ions.

The authors would like to acknowledge the Sudan Government for the award of a scholarship to BMM to allow him to study at the University of Sheffield.

References

- 1 C. M. George, in *Structure and Performance of Cements*, ed. P. Barnes, Applied Science, London, 1983, p. 415.
- 2 A. A. Goktas and M. C. Weinberg, *J. Am. Ceram. Soc.*, 1991, **74**, 1066.
- 3 F. T. Wallenberger, N. E. Weston and S. D. Brown, *Proc. Soc. Photo-Opt. Instrum. Eng., Int. Soc. Opt. Eng., Bellingham, WA*, 1991, **1484**, 116.
- 4 J. D. Birchall, A. J. Howard and K. Kendall, *Nature (London)*, 1981, **289**, 388.
- 5 J. Williamson and F. P. Glasser, *J. Appl. Chem.*, 1962, **12**, 535.
- 6 A. N. Scian, J. M. Porto Lopez and E. Pereira, *Cem. Concr. Res.*, 1987, **17**, 525.
- 7 V. K. Singh, M. M. Ali and U. K. Mandal, *J. Am. Ceram. Soc.*, 1990, **73**, 872.
- 8 K. I. Repenko, *Sb. Nauch. Tr. Ukr. Nauchn. Issled. Inst. Ogneuporeu*, 1963, **7**, 318.
- 9 K. S. Chou and G. Burnet, *Cem. Concr. Res.*, 1981, **11**, 167.
- 10 R. J. Gibbs, *Am. Mineral*, 1965, **50**, 741.
- 11 J. H. Sharp, G. W. Brindley and B. N. N. Achar, *J. Am. Ceram. Soc.*, 1966, **49**, 379.
- 12 M. Ayrami, *J. Chem. Phys.*, 1941, **9**, 177.
- 13 B. V. Erofe'ev, *Compt. Rend. Acad. Sci. URSS*, 1972, **52**, 74.
- 14 A. M. Ginstling and B. I. Brounshtein, *J. Appl. Chem. USSR*, 1950, **23**, 1327.
- 15 J. D. Hancock and J. H. Sharp, *J. Am. Ceram. Soc.*, 1972, **55**, 74.
- 16 M. A. Gulgun, O. O. Popoola and W. M. Kriven, *J. Am. Ceram. Soc.*, 1994, **77**, 531.

Paper 7/00201G; Received 8th January, 1997